RESEARCH ARTICLE

WILEY

Brain network hierarchy reorganization in Alzheimer's disease: A resting-state functional magnetic resonance imaging study

Qili Hu[1] ⓘ | Yunfei Li[1] | Yunying Wu[2,3] | Xiaomei Lin[1] | Xiaohu Zhao[1]

[1]Department of Imaging, The Fifth People's Hospital of Shanghai, Fudan University, Shanghai, China

[2]Bio-X Laboratory, Department of Physics, Zhejiang University, Hangzhou, China

[3]Center for Cognition and Brain Disorders, The Affiliated Hospital of Hangzhou Normal University, Hangzhou, China

Correspondence
Xiaohu Zhao, Department of Imaging, The Fifth People's Hospital of Shanghai, Fudan University, No. 128 Ruili Road, Minhang District, Shanghai 201100, China.
Email: xhzhao999@263.net

Abstract

Hierarchy is a fundamental organizational principle of the human brain network. Whether and how the network hierarchy changes in Alzheimer's disease (AD) remains unclear. To explore brain network hierarchy alterations in AD and their clinical relevance. Forty-nine healthy controls (HCs), 49 patients with mild cognitive impairment (MCI), and 49 patients with AD were included. The brain network hierarchy of each group was depicted by connectome gradient analyses. We assessed the network hierarchy changes by comparing the gradient values in each network across the AD, MCI, and HC groups. Whole-brain voxel-level gradient values were compared across the AD, MCI, and HC groups to identify abnormal brain regions. Finally, we examined the relationships between altered gradient values and clinical features. In the secondary gradient, the posterior default mode network (DMN) gradient values decreased significantly in patients with AD compared with HCs. Regionally, compared with HCs, both MCI and AD groups showed that most of the brain regions with increased gradient values were located in anterior DMN, while most of the brain regions with decreased gradient values were located in posterior DMN. The decrease of gradients in the left middle occipital gyrus was associated with better logical memory performance. The increase of gradients in the right middle frontal gyrus was associated with lower rates of dementia. The network hierarchy changed characteristically in patients with AD and was closely related to memory function and disease severity. These results provide a novel view for further understanding the underlying neuro-mechanisms of AD.

KEYWORDS
Alzheimer's disease, connectome gradient, default network, network hierarchy

Abbreviations: ACC, anterior cingulum; AD, Alzheimer's disease; aDMN, anterior default mode network; ANG, angular gyrus; CDR-SOB scores, Clinical Dementia Rating Scale-Sum of Boxes scores; DMN, default mode network; HC, healthy control; MCI, mild cognitive impairment; MFG, middle frontal gyrus; MFGtriang, triangular part of the inferior frontal gyrus; MNI, Montreal Neurological Institute; MOG, middle occipital gyrus; MRI, magnetic resonance imaging; MTG, middle temporal gyrus; OFC, orbital part of the medial frontal cortex; PCG, posterior cingulate gyrus.; pDMN, posterior default mode network; rs-fMRI, resting-state functional MRI.

1 | INTRODUCTION

Alzheimer's disease (AD), accounting for 60%–80% of all dementia cases, is an irreversible neurodegenerative disease (Dai & He, 2014). It has been reported that the number of people aged

65 and older with AD may grow to a projected 13.8 million by 2050 (https://www.alz.org). However, its pathogenesis is still unclear, and no effective therapeutic interventions are found currently. Mild cognitive impairment (MCI) is generally considered a transitional state between normal cognitive functioning and dementia (Belleville et al., 2011; Buschert et al., 2011; Busse et al., 2006; Ishikawa & Ikeda, 2007). The study of MCI is necessary for further exploration of AD.

The human cortex is organized as multiple large-scale networks, such as the sensorimotor network, visual network, and default-mode network (DMN) (Buckner & Krienen, 2013). Classical neuroanatomy and brain imaging have provided convergent support for the emergence of brain network hierarchy, with primary sensory networks at the bottom of the hierarchy, the DMN at the top of the hierarchy, and other networks spatially interspersed between the two (Cai et al., 2020; Margulies et al., 2016; Mesulam, 1998). Network hierarchy is thought to facilitate abstract, higher-order cognitive functions by helping segregate information that reflects the processing of the immediate environment from more self-generated operations emerging in high-level integrative networks (Lanzoni et al., 2020; Mesulam, 1998; Murphy et al., 2019).

Recent studies utilizing the connectome gradient analyses have revealed a principal gradient of network organization along the cortical surface (Margulies et al., 2016). This macroscale gradient is anchored at one end by the primary sensory network and at the other by the DMN, which reflects the cortical network hierarchy established in previous studies (Huntenburg et al., 2018). Studies using this technique have found that many neuropsychiatric diseases, including autism spectrum disorder, schizophrenia, and seizures, have abnormal network hierarchy changes (Bayrak et al., 2019; Dong et al., 2020; Hong et al., 2019) that are closely related to their clinical symptoms.

A large number of studies have demonstrated that AD involves extensive network abnormalities (Filippi et al., 2020; Ma et al., 2021; Veitch et al., 2019; Zott et al., 2018). However, previous studies have often defined discrete boundaries for each network and focused on functional abnormalities. Network hierarchy analyses can capture how these networks assemble together from a more integrative perspective (Bayrak et al., 2019). Exploring global network hierarchy alterations in patients with AD and MCI provides complementary information to previous studies and may be helpful in better understanding the pathogenesis of AD.

In the current study, we first mapped the network hierarchy pattern in the AD, MCI, and healthy control (HC) groups by using connectome gradient analyses. To assess the changes in network hierarchy in those with AD, we compared the gradient values between the AD and HC groups at the network level. Furthermore, whole-brain voxel-level comparisons were conducted to identify abnormal brain regions. Finally, we examined the relationship between altered gradient values and clinical features.

2 | METHODS

2.1 | Participants

Data used in the preparation of this article were obtained from the Alzheimer's Disease Neuroimaging Initiative database (available at https://adni.loni.usc.edu). The ADNI was launched in 2003 as a public-private partnership, led by Principal Investigator Michael W. Weiner, MD. The primary goal of the ADNI has been to test whether serial magnetic resonance imaging (MRI), positron emission tomography, other biologic markers, and clinical and neuropsychological assessments can be combined to assess the progression of MCI and early AD. Written informed consent was obtained from all individuals. Imaging data collected from 147 subjects were included in this study. The selection process for the participants is shown in the flowchart (Figure S1). Subjects were categorized into three groups: HCs ($n = 49$; age range: 57–91 years; mean age: 74.43 ± 8.24 years; 21 men), patients with MCI ($n = 49$; age range: 56–93; mean age: 73.35 ± 8.54 years; 27 men), and patients with AD ($n = 49$; age range: 55–95; mean age: 76.22 ± 8.54 years; 33 men). Details of the diagnostic criteria can be found at http://adni.loni.usc.edu/methods/documents/.

2.2 | Data acquisition and preprocessing

Resting-state functional MRI (rs-fMRI) images were obtained from all sites using a 3.0-T MRI scanner. For each subject, the first available rs-fMRI scan was used for the analysis. Detailed imaging protocols and scanning parameters can be found at http://adni.loni.usc.edu/methods/documents/. All preprocessing steps were carried out using the Data Processing & Analysis for (Resting-State) Brain Imaging and MATLAB scripts. The resting-state data were preprocessed using the following steps: (1) discard the first five volumes, (2) slice-time correct, (3) realign, (4) spatially normalize the images to the standard EPI template based on the Montreal Neurological Institute (MNI) stereotactic space. For computational efficiency, whole brain voxels were downsampled to 14000 voxels per hemisphere by resampling the image into 4 mm × 4 mm × 4 mm cubic voxels. (5) Data were spatially smoothed with a 6 mm × 6 mm × 6 mm full-width at half-maximum (FWHW) Gaussian kernel to decrease spatial noise, (6) detrended, (7) nuisance covariates, including Friston 24 head motion parameters, white matter signals, global mean signals, and cerebrospinal fluid signals were regressed out, (8) filtered using a bandpass filter (0.01–0.1 Hz).

2.3 | Connectivity gradient mapping analyses

We generated cortex-wide connectome gradients for each participant based on open software (https://github.com/NeuroanatomyAndConnectivity/gradient_analysis). Using the rs-fMRI time-series matrix

in each subject, we calculated the functional connectome based on systematic Pearson correlations (with 28454 × 28454 entries). Fisher's z-transformed and thresholder were further applied to the matrix, leaving only the top 10% of weighted connections per row, and a cosine similarity matrix that captured the similarity in the connectivity profiles between voxels was calculated. We applied the diffusion map embedding method to identify the various gradient components that explained the connectome variance in descending order (each of $1 \times 28,454$). In brief, the algorithm is a nonlinear dimensionality reduction technique that allowed us to identify gradients in the connectivity patterns based on the similarity matrix. In this way, the diffusion embedding result is not a single mosaic of discrete networks, but rather multiple continuous maps (gradients) that capture the similarity of each voxel's functional connections along a continuous space. In this space, cortical voxels that are strongly interconnected by either many connections or a few very strong connections are closer together, whereas voxels with little or no interconnectivity are farther apart. First, we calculated the average functional connection matrices of the AD, MCI, and HC groups based on all the subjects within each group. Each group's gradient pattern was obtained from its corresponding average connectivity matrix by using the diffusion map embedding method. For subject-wise alignment, we estimate a group-level gradient component template, generated from an average connectivity matrix based on subjects from all participants. Then, we performed Procrustes rotations to align the components of each individual to the template. These components, which were initially defined in MNI space, were mapped to the cortical surface to visualize macroscale transitions in the overall connectivity patterns.

2.4 | Network-level gradient comparison across the AD, MCI, and HC groups

The connectome gradient mapping results showed that in the secondary gradient, all groups had a continuum of connectivity variation, ranging from low-level sensory systems to the trans-modal DMN, with the remaining networks falling somewhere in between, which reflected the hierarchical distribution pattern of brain networks. To investigate network hierarchy changes in patients with AD and MCI, our subsequent analysis mainly focused on the secondary gradient. To assess the brain network hierarchy changes in those with AD, we compared the gradient values in each subnetwork between the AD and CN, AD and MCI, and MCI and CN groups. For the resting-state maps, we used the MNI-space version ("liberal mask") of the seven network parcellations (sensorimotor network, visual network, dorsal attention network, ventral attention network, limbic network, frontoparietal network, and DMN) by Yeo et al. (2011) (Yeo et al., 2011). According to previous anatomical, independent component analysis and functional connectivity results (Cai et al., 2020; Jones et al., 2011; Xue et al., 2019), we further separated the DMN into the anterior DMN (aDMN) and posterior DMN (pDMN). The average gradient values of each subnetwork in the AD, MCI, and HC groups were calculated. We examined the between-group differences

by using two-sample t tests. A linear regression analysis (controlling for sex and years of education) was used. The regression results were presented in Supporting Information (Figure S2).

2.5 | Whole-brain voxel-level gradient comparison across the AD, MCI, and HC groups

To further identify regions with brain hierarchy changes, we compared the gradient values of each voxel between the AD and CN, AD and MCI, and MCI and CN groups using two-sample t tests. A linear regression analysis (controlling for sex and years of education) was used. The regression results were presented in Supporting Information (Figure S3). The AlphaSim correction (p <.05 at both voxel and cluster level, http://afni.nif.gov/afni/docpdf/AlphaSim.pdf) was used for multiple comparisons. To increase the credibility of our results, we also applied GRF correction for multiple corrections (two-tailed, voxel level p <.05, cluster level p <.05). For the exploration analysis in the principle gradient, gradient values of each voxel between the AD and CN, AD, and MCI groups were compared using two-sample t tests (uncorrected both p <.05 and p <.01).

2.6 | Correlations between altered gradient scores and clinical variables

The Harvard-Oxford cortical and subcortical structural atlases were used to parcellate the brain cortex into 110 regions of interest. The Clinical Dementia Rating Scale (CDR) Sum of Boxes (SOB) quantifies dementia severity and progression in clinical AD trials. Logical memory is a commonly used measure of verbal memory. Previous studies have found that logical memory measures are sensitive to early memory impairment in patients with AD, and it is helpful for distinguishing MCI from Alzheimer's disease (Mueller et al., 2020; Orimaye et al., 2020). We extracted the average gradient value of overlapping regions of interest (ROIs) and clusters (extracted based on a voxel-based threshold with AlphaSim correction, defining the minimum cluster extent as 392.7 voxels) and performed a correlation analysis between this value and the CDR-SOB and logical memory scores with Pearson's correlations. In the exploration of the principal gradient, we did not use the Harvard-Oxford template. The average gradient values of the clusters were analyzed for their correlation with the CDR-SOB and logical memory scores using Pearson's correlations.

2.7 | Validation analysis

We recruited an independent sample set to validate our results. This independent dataset was composed of young individuals in Human Connectome Project datasets ($n = 49$; 18 males and 31 females; age 22–35 years). Since the TR of HCP fMRI is very short due to the multiband nature of the acquisition, the value of the slice timing correction is limited. Therefore, we repeated the whole processing

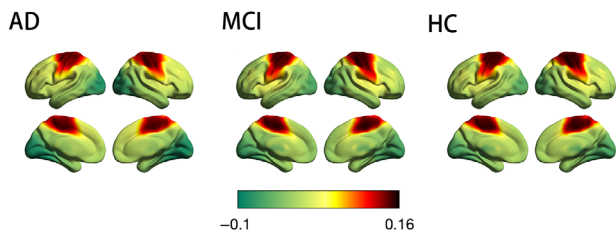**TABLE 1** Demographics and clinical information

Characteristics	Healthy control (n = 49)	Mild cognitive impairment (n = 49)	Alzheimer's disease (n = 49)	p-value
Age (year)	74.43 ± 8.24	73.35 ± 8.54	76.22 ± 8.54	.259[a]
Education (year)	16.94 ± 2.32	16.22 ± 1.83	16.73 ± 2.78	.093[a]
Sex (M/F)	21/28	27/22	33/16	.051[b]
MMSE	29.04 ± 1.14	28.10 ± 1.60	21.92 ± 2.94	.000[a]
LM	14.59 ± 3.69	8.57 ± 4.16	1.45 ± 2.17	.000[a]

Note: Data are presented as the means ± standard deviation (SD).
[a]*p* value obtained by a Kruskal–Wallis H test.
[b]*p* value obtained by a two-tailed Pearson chi-square test.
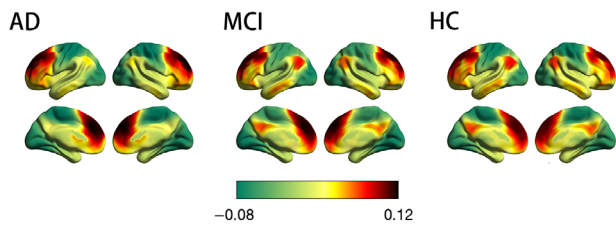

FIGURE 1 Connectome gradient mapping in the Alzheimer's disease (AD), mild cognitive impairment (MCI), and healthy control (HC) groups. (a) and (b) show the principal and secondary gradient mapping results, respectively. The scale bar reflects z-transformed gradient values derived from connectivity matrices using diffusion map embedding. The proximity of colors indicates the similarity in connectivity patterns across the cortex. (a) The principal gradient of connectivity in the AD, MCI, and HC groups peaks within primary sensory networks, separating somatomotor network regions (red) from visual network regions (green). (b) The secondary gradient shows a gradual axis of connectivity variations that placed low-level sensory network regions (green) on the one end and high-level default mode network regions (red) on the other end, with intermediary network regions in between

FIGURE 2 Network-level secondary gradient comparison between Alzheimer's disease (AD) and healthy control (HC) groups. The radar chart shows the gradient Z-score (with respect to HCs) of the two groups. In the secondary gradient, compared to HCs, patients with AD exhibited significantly lower gradient values in the pDMN (Cohen's d = −0.53, t = −2.6399, p = .0097). There were no differences in gradient values between patients with AD and HCs in the remaining subnetworks. Each subnetwork's spatial location was anchored in the corresponding position, and Cohen's d was computed among the groups. The IDs of subjects included in the final analyses were provided in Table.S1.

pipeline (except slice timing) with the same parameters and compared the gradient mapping pattern from the previous gradient analysis to that in young individuals.

3 | RESULTS

3.1 | Clinical and demographic characteristic comparisons

The clinical and demographic data of the 147 subjects were shown in Table 1. There were no significant differences in sex, age or education
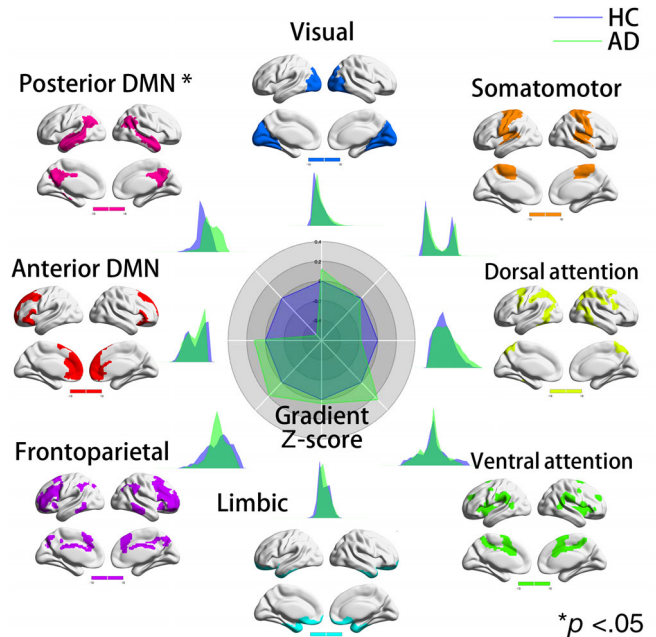
3.2 | Principal and secondary gradient patterns in the AD, MCI, and HC groups

The principal and secondary gradients explained 23% and 16% of the whole-brain connectome variance across the AD, MCI, and HC subjects, respectively (Figure S4). The variances explained by the principal and secondary gradients between the three groups were not significantly different (analysis of variance with age as a regression variable: $F = 0.38$, $p = .54$ for the principal gradient; $F = 0.18$, $p = .67$ for the
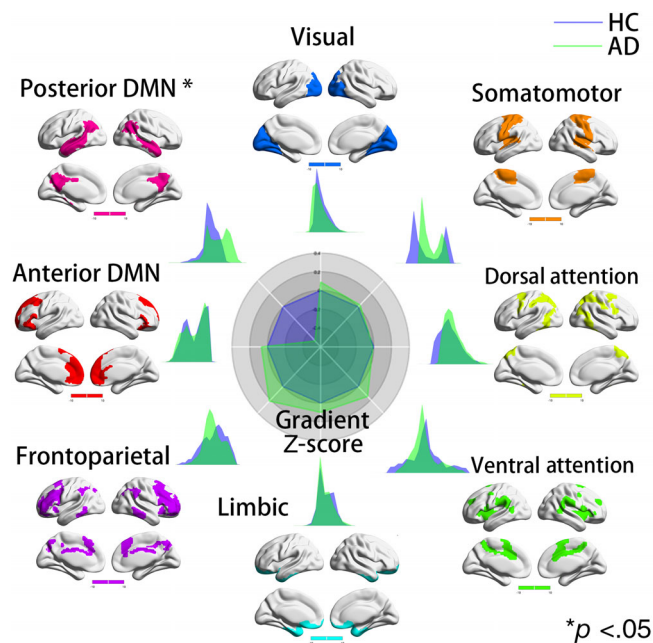
FIGURE 3 Network-level secondary gradient comparison between Alzheimer's disease (AD) and mild cognitive impairment (MCI) groups. The radar chart shows the gradient Z-score (with respect to MCI) of the two groups. In the secondary gradient, compared with patients with MCI, patients with AD had significantly lower pDMN gradient values (Cohen's $d = -0.51$, $t = -2.5311$, $p = .013$), which was consistent with the network-level gradient comparison result between the AD and healthy control (HC) groups. There were no differences in gradient values between patients with AD and MCI in the remaining subnetworks. Each subnetwork's spatial location was anchored in the corresponding position, and Cohen's d was computed

FIGURE 4 Whole-brain voxel-level secondary gradient comparisons among the Alzheimer's disease (AD), mild cognitive impairment (MCI), and healthy control (HC) groups with AlphaSim correction. Blue and red clusters denote regions with significantly decreased and increased gradients, respectively ($p < .05$, cluster size ≥392.7 voxels, Alphasim corrected). Compared with HCs, patients with AD exhibited significant functional gradient increases mainly in the bilateral MFG, OFC, MFGtriang, and ACC, and decreases mainly in the bilateral ANG, MOG, MTG, and PCUN/PCG. Compared with patients with MCI, patients with AD exhibited a similar gradient changing pattern, showing significant increase of gradient values mainly in the MFG.R, OFC.R, MFGtriang.R, insula.R, and the bilateral ACC and decrease mainly in bilateral ANG, MTG, and PCG. There were no differences between patients with MCI and HCs in gradient values after correction

secondary gradient). We found that the first two gradient patterns differed from previous findings in young individuals. The principal gradient was anchored between the sensorimotor and visual networks, which closely resembled the secondary gradient previously identified in adults (Margulies et al., 2016). The secondary gradient showed a gradual axis of connectivity variations, with low-level sensory networks on one end and high-level DMN on the other, with intermediary networks in between, similar to the principal gradient previously identified in adults (Figure 1). The gradient patterns of the groups were plotted in the gradient space marked by the principal gradient and secondary gradient (Figure S5).

3.3 | Network-level gradient comparison among the AD, MCI, and HC groups

In the secondary gradient, compared to HCs, patients with AD exhibited significantly lower gradient values in the pDMN (Cohen's $d = -0.53$, $t = -2.6399$, $p = .0097$) (Figure 2). There were no differences in gradient values between patients with AD and HCs in the remaining subnetworks. Compa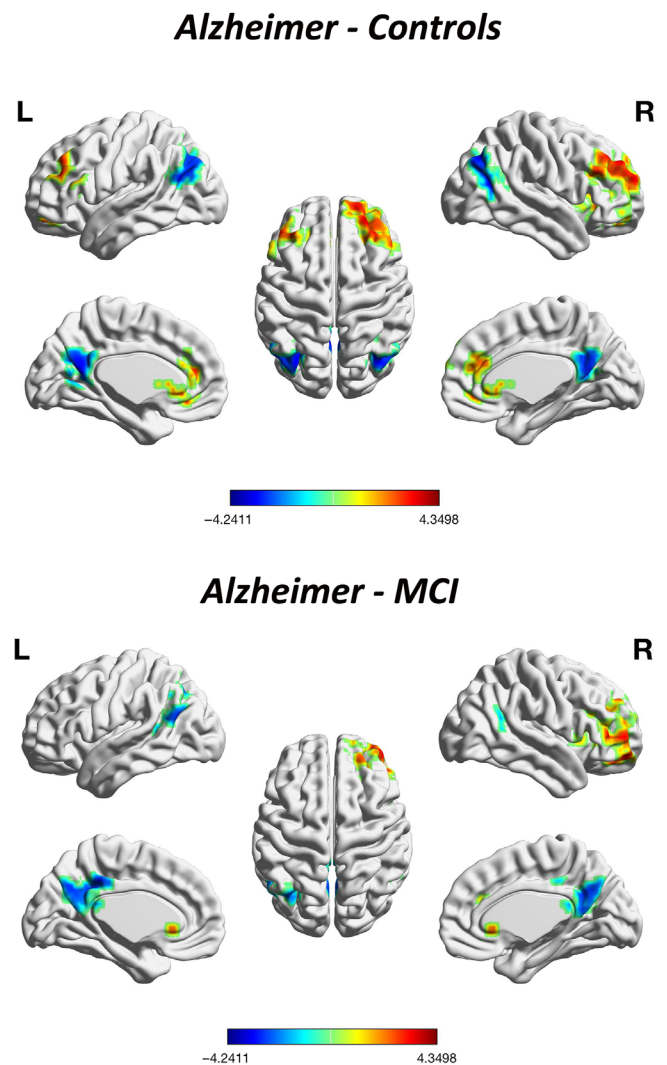red with patients with MCI, patients with AD had significantly lower pDMN gradient values (Cohen's $d = -0.51$, $t = -2.5311$, $p = .013$; Figure 3), which was consistent with the network-level gradient comparison result between the AD and HC groups. There were no differences in gradient values between patients with AD and MCI in the remaining subnetworks. There were no differences in gradient values between patients with MCI and HCs in the seven subnetworks (Figure S6).

TABLE 2 Differences in secondary gradient values between Alzheimer's disease (AD) patients and healthy controls (HCs) after AlphaSim correction

Comparison	Cluster size	Peak value	Peak coordinates
AD-HCs			
	890	4.35	[30, 50, 40]
	679	−4.24	[−34, −70, 32]
AD-MCI			
	432	4.20	[46, 50, 4]
	408	−3.31	[−6, −38, 40]

3.4 | Whole-brain voxel-level secondary gradient comparisons among the AD, MCI, and HC groups

Compared with HCs, patients with AD showed that most of the brain regions with increased gradient values were located in aDMN, while most of the brain regions with decreased gradient values were located in pDMN. The dorsal prefrontal cortex (dlPFC) regions including bilateral middle frontal gyrus (MFG), orbital part of the medial frontal cortex (OFC), triangular part of the inferior frontal gyrus (MFGtriang) as well as insula and anterior cingulum (ACC) showed an increase in gradient value. The bilateral middle occipital gyrus (MOG), middle temporal gyrus (MTG), angular gyrus (ANG), and posterior cingulate gyrus. (PCG) showed a decrease in gradient value (p <.05, cluster size ≥392.7 voxels, AlphaSim corrected). When compared with MCI patients, AD patients exhibited a similar gradient changing pattern, with a significant increase in gradient values mainly in the MFG.R, OFC.R, MFGtriang.R, insula.R, and the bilateral ACC, and decreases in the bilateral ANG, MTG, and PCG (p <.05, cluster size ≥392.7 voxels, AlphaSim corrected; Figure 4). There were no differences in gradient values between patients with MCI and HCs after both AlphaSim corrections. The cluster size, peak coordinates, and T-statistics of the results of voxel-wise gradient value AD-CN, AD-MCI, and MCI-CN comparisons was provided in Table 2. With GRF correction, compared with HCs, AD patients showed similar brain regions with gradient value changes to those with Alphasim correction, showing significant functional gradient increases mainly in the MFG.R and decreases mainly in the MOG.L and bilateral PCUN/ PCG (p <.05, GRF corrected; Figure S7). There were no differences in gradient values between MCI and HC groups as well as AD groups after both GRF corrections.

3.5 | Correlations between altered secondary gradient values and clinical variables

In patients with AD, the CDR-SOB scores were negatively correlated with the gradient values in the MFG.R (p = .046). The logical memory scores were negatively correlated with the functional gradient values in the MOG.L (p = .046; Figure 5).

3.6 | Altered principal gradient values in AD and MCI and correlations with clinical variables

Exploratory analyses were also conducted to explore the regions with altered principal gradients and their correlations with clinical variables. Voxel-wise comparisons revealed that, compared with both HC and MCI groups, the AD group showed a significant gradient increase in the bilateral thalamus (p <.05, uncorrected). The cluster size, peak coordinates, and T-statistics of the results of voxel-wise gradient value AD-CN, AD-MCI, and MCI-CN comparisons was provided in Table 3. Furthermore, the gradient values in the bilateral thalamus were positively correlated with CDR-SOB scores and negatively correlated with logical memory scores in AD patients (p = .048, p = .040; Figure 6). To increase the credibility of our results, we also performed the voxel-level principle gradient comparison across the three groups with the p-value<.01. The gradient comparison results with the p-value <.01 were similar to the results with the p-value <.05. Compared with both HC and MCI groups, the AD group showed a significant gradient increase in the bilateral thalamus (Figure S8).

3.7 | Validation analysis with young individuals

The principal gradient in young individuals showed a gradual axis of connectivity variations, with low-level sensory networks on one end and high-level DMN on the other, which resembled the principal gradient previously identified in adults (Figure S9). This confirmed that there were no calculation errors in our study and further supports our findings.

4 | DISCUSSION

Hierarchy is a fundamental organizational principle of the human brain networks. Whether and how network hierarchy changes in AD remains unclear. Our research results can be summarized as follows. (1) The pDMN gradient values decreased significantly in patients with AD compared with HCs. (2) Specifically, compared with HCs, patients with AD exhibited a higher gradient value in the MFG.R of the FPN and a lower gradient value mainly in the pDMN regions, including the bilateral MTG, PCG, ANG, and MOG. (3) The decrease in the gradient value of the MOG.L in the pDMN is associated with better logical memory performance. The increase in the gradient value of the MFG. R in the FPN is associated with lower rates of clinical dementia. Additionally, it is worth noting that when compared with previous results established in adults, the principal and secondary gradients were reversed in the AD, MCI, and HC groups. These findings warrant additional in-depth studies in future work.

Our results showed that the pDMN hierarchy, or the so-called network gradient, decreased more noticeably in patients with AD than in HCs or patients with MCI, which reflects decreased segregation between the pDMN and the remaining networks. The DMN is associated with high-level cognitive function (Buckner & DiNicola, 2019). It
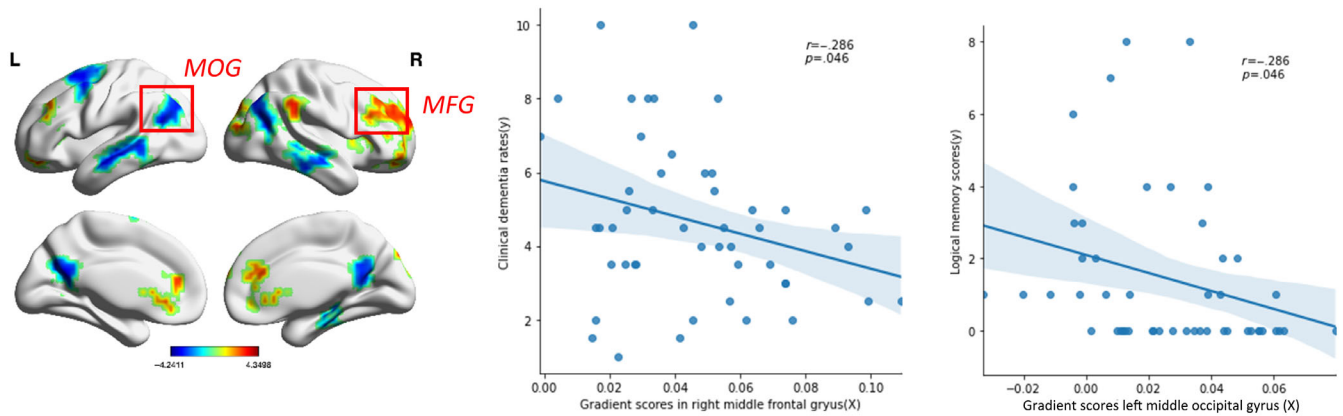
FIGURE 5 Correlations between secondary gradient values and clinical variables. (a) The clinical dementia rating scores and functional gradient values in the MFG.R (p <.05) were negatively correlated. (b) The logical memory scores and functional gradient values in the MOG.L were negatively correlated (p <.05). Clinical data from 49 AD patients were used in the Pearson correlation analyses

TABLE 3 Differences in principal gradient values between Alzheimer's disease (AD) patients and healthy controls (HCs) without correction

Comparison	Cluster size	Peak value	Peak coordinates
AD-HCs			
	801	3.93	[−22, −50, −60]
	52	3.640	[6, 62, −24]
	69	3.182	[−54, −50, −12]
	98	3.69	[−30, −94, −4]
	87	4.18	[−2, −22, 8]
	77	3.28	[−38, 26, 12]
	69	3.23	[−14, −78, 32]
	59	−3.36	[22, −74, 28]
AD-MCI			
	395	4.21	[6, −58, −52]
	110	−3.39	[−50, −78, 0]
	119	3.63	[−2, −22, 8]
	107	−3.48	[−30, 18, 8]
	91	−3.40	[−66, −14, 20]
MCI-HCs			
	145	−3.30	[26, −54, 40]

can be further divided into the aDMN and the pDMN. The aDMN is associated with social cognitive functions, such as affective self-referential processing and inferring others' mental states, whereas the pDMN is related to several cognitive processes, including temporal episodic memory and thinking about the future (Wang et al., 2018; Yang et al., 2017). Dysfunction in the pDMN has been widely reported and is thought to be involved in the physiopathology of memory impairment and other cognitive dysfunctions in patients with AD (Ibrahim et al., 2021; Mandal et al., 2018). When analyzing task-free data, Jones et al. (2011) found that, when compared with cognitively normal controls, subjects with AD showed decreased functional

connectivity in the pDMN. Cai et al. (2020) found that patients with MCI showed distinct phase position connectivity alternations in DMN subnetworks, which may contribute to varying degrees of MCI across the AD spectrum. Consistent with these results, the current study found that gradient changes mainly occurred in the pDMN, which provides further support for the important role of the pDMN in AD.

More importantly, network hierarchy provides a novel perspective for exploring the underlying neuro-mechanisms of AD. Network hierarchy has been widely recognized as a key principle of human brain organization that controls a set of cognitive functions. Recent studies have found that many neuropsychiatric diseases have abnormal network hierarchy changes. Hong et al. (2019) found that, when compared with typically developing controls, patients with autism spectrum disorder showed a reduced gradient distance between the DMN and the primary sensory networks, which was associated with deficits in low-level symptoms and high-level cognition. Another study (Dong et al., 2020) indicated that patients with schizophrenia showed increased gradient values in SMN regions and decreased gradient values in DMN regions, which was correlated with the severity of negative symptoms and the duration of the illness. In the current work, we found that the pDMN gradient was significantly decreased in patients with AD, which may be related to the pathological changes associated with AD and is promising as a novel biomarker for AD diagnosis and prognosis.

Regionally, compared with HCs, both MCI and AD patients showed that most of the brain regions with increased gradient values were located in aDMN, while most of the brain regions with decreased gradient values were located in pDMN. Besides, we found that the gradient values within MOG, which situated in visual network were also significantly decreased. These results reflected the enhanced separation between primary visual network and high-level cognitive network as well as between aDMN and pDMN in AD. Further correlation analysis showed that the increase in the gradient value of the MFG.R was related to lower dementia rates. The decrease in the gradient value of the left MOG.L is related to better logical memory performance. Previous study demonstrated that the
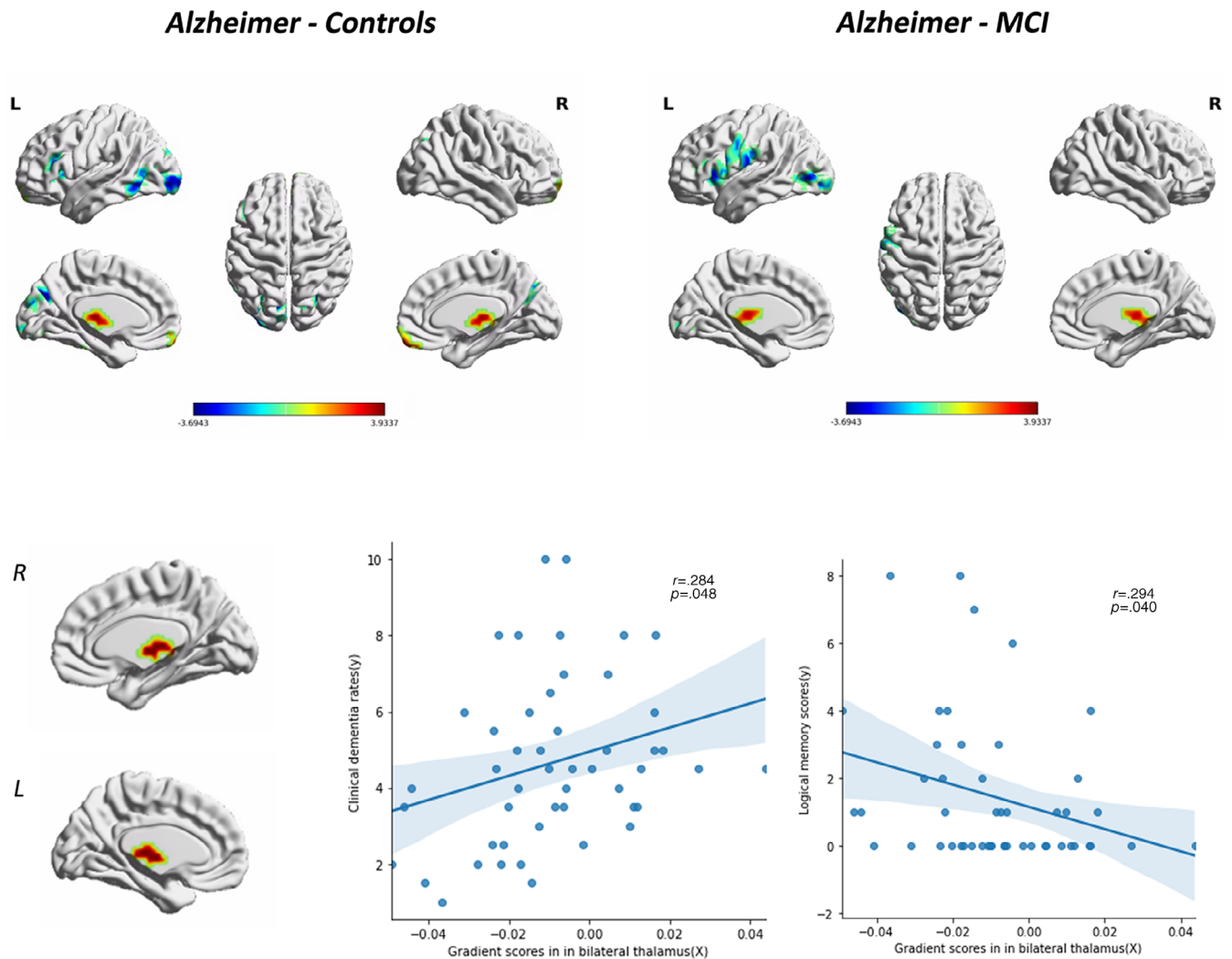
FIGURE 6 Altered principal gradient values in Alzheimer's disease (AD) group and correlations with clinical variables. Compared with both healthy control (HC) and mild cognitive impairment (MCI) groups, AD group showed a significant gradient increase in bilateral thalamus. The gradient values of bilateral thalamus were positively correlated with CDR-SOB scores and negatively correlated with logical memory performance in AD patients ($p < .05$). Clinical data from 49 AD patients were used in the Pearson correlation analyses

inherent segregation of brain network organization is helpful for facilitating higher-order cognition (Hong et al., 2019; Murphy et al., 2019). We speculate cautiously that the gradient value change in these regions found in AD group may serve as a compensatory strategy of patients for maintaining cognitive functions.

Additionally, we found that, when compared with previous results established in adults, the principal and secondary gradient patterns in the AD, MCI, and HC groups were switched. A recent study also found that the first two gradient patterns were switched in children (age 7–14; Dong et al., 2021). Another study including 170 people between the ages of 17 and 87 found that the gradient values in the DMN, FPN, and dorsal attention network gradually changed with increasing age (Bethlehem et al., 2020). The results suggest that network distribution patterns in the principal and secondary gradients differ in children, teenagers, and elderly individuals. The subjects in the AD, MCI, and HC groups were all over 75 years old on average. We suspect that the characteristic principal and secondary gradient

pattern differences between our results and those of previous studies may be attributable to age. To eliminate methodological errors, we recruited another independent sample set of young individuals ($n = 49$; age 22–35) from the Human Connectome Project and repeated the whole processing pipeline with the same parameters. We found that the gradient pattern was similar to previous results, which further supports our speculation. The gradient pattern changes across different age groups warrant further study in future work.

A limitation of our study is that we did not explore changes in the subcortical–cortical gradient patterns. Our understanding of subcortical structure involvement in brain disorders has evolved from motor processing to high-level cognitive and affective processing. The thalamic system has extensive projections to cerebral functional networks and plays a critical role in the pathology of AD (Zhao et al., 2021). The current study found that the principal gradient values in the bilateral thalamus significantly increased in patients with AD and were closely correlated with cognitive functions. The gradients of the thalamus may provide a

good system for better understanding the pathophysiology of AD and should be studied further.

5 | CONCLUSION

In summary, the current study found characteristic network hierarchy reorganization patterns in patients with AD that were closely related to memory function and disease severity. These results provide a novel view for further understanding the underlying neuro-mechanisms of AD.

CONFLICT OF INTEREST

The authors declare no potential conflict of interest.

AUTHOR CONTRIBUTIONS

Guarantors of integrity of entire study: Xiaohu Zhao; *Study concepts/ study design or data acquisition or data analysis/interpretation*: Qili Hu and Yunying Wu; *Manuscript drafting or manuscript revision for important intellectual content*: Qili Hu; *Approval of final version of submitted manuscript*: all authors; *Agrees to ensure any questions related to the work are appropriately resolved*: all authors; *Literature research*: Xiaomei Lin; *Clinical studies*: Yunfei Li; *Experimental studies*: Yunfei Li; *And manuscript editing*: Yunfei Li.

DATA AVAILABILITY STATEMENT

The data that support the findings of this study are openly available at http://adni.loni.usc.edu/.

ORCID

Qili Hu https://orcid.org/0000-0002-4088-1063

REFERENCES

Bayrak, Ş., Khalil, A., Villringer, K., Fiebach, J., Villringer, A., Margulies, D., & Ovadia-Caro, S. (2019). The impact of ischemic stroke on connectivity gradients. *NeuroImage: Clinical*, *24*, 101947. https://doi.org/10.1016/j.nicl.2019.101947

Belleville, S., Clément, F., Mellah, S., Gilbert, B., Fontaine, F., & Gauthier, S. (2011). Training-related brain plasticity in subjects at risk of developing Alzheimer's disease. *Brain*, *134*, 1623–1634. https://doi.org/10.1093/brain/awr037

Bethlehem, R., Paquola, C., Seidlitz, J., Ronan, L., Bernhardt, B., Consortium, C., & Tsvetanov, K. J. N. (2020). Dispersion of functional gradients across the adult lifespan. *NeuroImage*, *222*, 117299. https://doi.org/10.1016/j.neuroimage.2020.117299

Buckner, R. L., & DiNicola, L. M. (2019). The brain's default network: Updated anatomy, physiology and evolving insights. *Nature Reviews. Neuroscience*, *20*(10), 593–608. https://doi.org/10.1038/s41583-019-0212-7

Buckner, R. L., & Krienen, F. M. (2013). The evolution of distributed association networks in the human brain. *Trends in Cognitive Sciences*, *17*(12), 648–665. https://doi.org/10.1016/j.tics.2013.09.017

Buschert, V., Friese, U., Teipel, S., Schneider, P., Merensky, W., Rujescu, D., Möller, H.-J., Hampel, H., & Buerger, K. (2011). Effects of a newly developed cognitive intervention in amnestic mild cognitive impairment and mild Alzheimer's disease: A pilot study. *Journal of Alzheimer's Disease*, *25*(4), 679–694. https://doi.org/10.3233/jad-2011-100999

Busse, A., Hensel, A., Gühne, U., Angermeyer, M., & Riedel-Heller, S. (2006). Mild cognitive impairment: Long-term course of four clinical subtypes. *Neurology*, *67*(12), 2176–2185. https://doi.org/10.1212/01.wnl.0000249117.23318.e1

Cai, C., Huang, C., Yang, C., Zhang, X., Peng, Y., Zhao, W., Hong, X., Ren, F., Hong, D., Xiao, Y., & Yan, J. (2020). Altered patterns of phase position connectivity in default mode subnetwork of subjective cognitive decline and amnestic mild cognitive impairment. *Frontiers in Neuroscience*, *14*, 185. https://doi.org/10.3389/fnins.2020.00185

Dai, Z., & He, Y. (2014). Disrupted structural and functional brain connectomes in mild cognitive impairment and Alzheimer's disease. *Neuroscience Bulletin*, *30*(2), 217–232. https://doi.org/10.1007/s12264-013-1421-0

Dong, D., Luo, C., Guell, X., Wang, Y., He, H., Duan, M., Eickhoff, S. B., & Yao, D. (2020). Compression of cerebellar functional gradients in Schizophrenia. *Schizophrenia Bulletin*, *46*, 1282–1295. https://doi.org/10.1093/schbul/sbaa016

Dong, H.-M., Margulies, D. S., Zuo, X.-N., & Holmes, A. J. (2021). Shifting gradients of macroscale cortical organization mark the transition from childhood to adolescence. *Psychological and Cognitive Sciences*, *118*(28), e2024448118. https://doi.org/10.1073/pnas.2024448118

Filippi, M., Basaia, S., Canu, E., Imperiale, F., Magnani, G., Falautano, M., Comi, G., Falini, A., & Agosta, F. (2020). Changes in functional and structural brain connectome along the Alzheimer's disease continuum. *Molecular Psychiatry*, *25*(1), 230–239. https://doi.org/10.1038/s41380-018-0067-8

Hong, S., de Wael, R. V., Bethlehem, R., Lariviere, S., Paquola, C., Valk, S., Milham, M. P., Di Martino, A., Margulies, D. S., Smallwood, J., & Bernhardt, B. C. (2019). Atypical functional connectome hierarchy in autism. *Nature Communications*, *10*(1), 1022. https://doi.org/10.1038/s41467-019-08944-1

Huntenburg, J., Bazin, P., & Margulies, D. S. (2018). Large-scale gradients in human cortical organization. *Trends in Cognitive Sciences*, *22*(1), 21–31. https://doi.org/10.1016/j.tics.2017.11.002

Ibrahim, B., Suppiah, S., Ibrahim, N., Mohamad, M., Hassan, H., Nasser, N., & Saripan, M. I. (2021). Diagnostic power of resting-state fMRI for detection of network connectivity in Alzheimer's disease and mild cognitive impairment: A systematic review. *Human Brain Mapping*, *42*(9), 2941–2968. https://doi.org/10.1002/hbm.25369

Ishikawa, T., & Ikeda, M. (2007). Mild cognitive impairment in a population-based epidemiological study. *Psychogeriatrics*, *7*(3), 104–108. https://doi.org/10.1111/j.1479-8301.2007.00197.x

Jones, D., Machulda, M., Vemuri, P., McDade, E., Zeng, G., Senjem, M., Gunter, J. L., Przybelski, S. A., Avula, R. T., Knopman, D. S., Boeve, B. F., Petersen, R. C., & Jack, C. R. (2011). Age-related changes in the default mode network are more advanced in Alzheimer disease. *Neurology*, *77*(16), 1524–1531. https://doi.org/10.1212/WNL.0b013e318233b33d

Lanzoni, L., Ravasio, D., Thompson, H., Vatansever, D., Margulies, D., Smallwood, J., & Jefferies, E. J. N. (2020). The role of default mode network in semantic cue integration. *Neuroimage*, *219*, 117019. https://doi.org/10.1016/j.neuroimage.2020.117019

Ma, W., Yao, Q., Hu, G., Ge, H., Xue, C., Wang, Y., Xiao, C.-Y., Shi, J.-P., & Chen, J. (2021). Reorganization of rich clubs in functional brain networks of dementia with Lewy bodies and Alzheimer's disease. *NeuroImage. Clinical*, *33*, 102930. https://doi.org/10.1016/j.nicl.2021.102930

Mandal, P., Banerjee, A., Tripathi, M., & Sharma, A. (2018). A comprehensive review of magnetoencephalography (MEG) studies for brain functionality in healthy aging and Alzheimer's disease (AD). *Frontiers in*

Computational Neuroscience, *12*, 60. https://doi.org/10.3389/fncom.2018.00060

Margulies, D., Ghosh, S., Goulas, A., Falkiewicz, M., Huntenburg, J., Langs, G., Bezgin, G., Eickhoff, S. B., Castellanos, F. X., Petrides, M., Jefferies, E., & Smallwood, J. (2016). Situating the default-mode network along a principal gradient of macroscale cortical organization. *Proceedings of the National Academy of Sciences of the United States of America*, *113*, 12574–12579.

Mesulam, M. M. (1998). From sensation to cognition. *Brain*, *121*, 1013–1052. https://doi.org/10.1093/brain/121.6.1013

Mueller, K., Koscik, R., Du, L., Bruno, D., Jonaitis, E., Koscik, A., Christian, B. T., Betthauser, T. J., Chin, N. A., Hermann, B. P., & Johnson, S. C. (2020). Proper names from story recall are associated with beta-amyloid in cognitively unimpaired adults at risk for Alzheimer's disease. *Cortex*, *131*, 137–150. https://doi.org/10.1016/j.cortex.2020.07.008

Murphy, C., Wang, H., Konu, D., Lowndes, R., Margulies, D., Jefferies, E., & Smallwood, J. (2019). Modes of operation: A topographic neural gradient supporting stimulus dependent and independent cognition. *Neuroimage*, *186*, 487–496. https://doi.org/10.1016/j.neuroimage.2018.11.009

Orimaye, S., Goodkin, K., Riaz, O., Salcedo, J., Al-Khateeb, T., Awujoola, A., & Sodeke, P. (2020). A machine learning-based linguistic battery for diagnosing mild cognitive impairment due to Alzheimer's disease. *PLoS One*, *15*(3), e0229460. https://doi.org/10.1371/journal.pone.0229460

Veitch, D., Weiner, M., Aisen, P., Beckett, L., Cairns, N., Green, R., Harvey, D., Jack, C. R., Jagust, W., Morris, J. C., Petersen, R. C., Saykin, A. J., Shaw, L. M., Toga, A. W., Trojanowski, J. Q., & Alzheimer's Disease Neuroimaging Initiative. (2019). Understanding disease progression and improving Alzheimer's disease clinical trials: Recent highlights from the Alzheimer's Disease Neuroimaging Initiative. *Alzheimers Dement*, *15*(1), 106–152. https://doi.org/10.1016/j.jalz.2018.08.005

Wang, C., Pan, Y., Liu, Y., Xu, K., Hao, L., Huang, F., Ke, J., Sheng, L. Q., Ma, H. R., & Guo, W. F. (2018). Aberrant default mode network in amnestic mild cognitive impairment: A meta-analysis of independent component analysis studies. *Neurological Sciences*, *39*(5), 919–931. https://doi.org/10.1007/s10072-018-3306-5

Xue, C., Yuan, B., Yue, Y., Xu, J., Wang, S., Wu, M., Ji, N., Zhou, X., Zhao, Y., Rao, J., Yang, W., Xiao, C., & Chen, J. (2019). Distinct disruptive patterns of default mode subnetwork connectivity across the Spectrum of preclinical Alzheimer's disease. *Frontiers in Aging Neuroscience*, *11*, 307. https://doi.org/10.3389/fnagi.2019.00307

Yang, H., Wang, C., Zhang, Y., Xia, L., Feng, Z., Li, D., Xu, S., Xie, H., Chen, F., Shi, Y., & Wang, J. (2017). Disrupted causal connectivity anchored in the posterior cingulate cortex in amnestic mild cognitive impairment. *Frontiers in Neurology*, *8*, 10. https://doi.org/10.3389/fneur.2017.00010

Yeo, B., Krienen, F., Sepulcre, J., Sabuncu, M., Lashkari, D., Hollinshead, M., Roffman, J. L., Smoller, J. W., Zöllei, L., Polimeni, J. R., Fischl, B., Liu, H., & Buckner, R. L. (2011). The organization of the human cerebral cortex estimated by intrinsic functional connectivity. *Journal of Neurophysiology*, *106*(3), 1125–1165. https://doi.org/10.1152/jn.00338.2011

Zhao, H., Cheng, J., Liu, T., Jiang, J., Koch, F., Sachdev, P. S., Basser, P. J., Wen, W., & Alzheimer's Disease Neuroimaging Initiative. (2021). Orientational changes of white matter fibers in Alzheimer's disease and amnestic mild cognitive impairment. *Human Brain Mapping*, *42*, 5397–5408. https://doi.org/10.1002/hbm.25628

Zott, B., Busche, M., Sperling, R., & Konnerth, A. (2018). What happens with the circuit in Alzheimer's disease in mice and humans? *Annual Review of Neuroscience*, *41*, 277–297. https://doi.org/10.1146/annurev-neuro-080317-061725

SUPPORTING INFORMATION

Additional supporting information may be found in the online version of the article at the publisher's website.